# Drift mobility of semiconductive $La_{0.5}Sr_{0.5}CoO_3$ films measured using the traveling wave method

J. Yin, L. Wang, J. M. Liu, K. J. Chen, and Z. G. Liu[a)]
*National Laboratory of Solid State Microstructures, Nanjing University, Nanjing 210093, People's Republic of China*

Q. Huang
*Department of Physics, National University of Singapore, Singapore 119260*

(Received 18 May 1999; accepted for publication 30 November 1999)

The conductivity and the drift mobility of $La_{0.5}Sr_{0.5}CoO_3$ films deposited on fused silica substrates at 650 °C by pulsed-laser deposition have been measured by using the traveling-wave method. At room temperature, $La_{0.5}Sr_{0.5}CoO_3$ films with semiconductivity have a hole density of $1\times10^{21}\,cm^{-3}$, and drift mobility of $0.01\,cm^2/V\,s$. The films underwent a paraferromagnetic transition around 240 K. The hopping process and tunneling effect of small polarons may be responsible for the conductive behavior above the Curie temperature. © *2000 American Institute of Physics.* [S0003-6951(00)01105-0]

The observation of giant magnetoresistance (GMR) has attracted great interest in studies on the electronic properties of doped $La_{1-x}A_xMnO_3$ (A=Sr,Ca,Ba,Pb) and other transition-metal oxides having strong electron correlations.[1–3] The substitution of $La^{3+}$ by $Sr^{2+}$ ions produces holes in the $e_g$ orbitals which are strongly hybridized with oxygen $2p$ states. The ferromagnetic interaction between localized $t_{2g}$ spin (spin quantum number $S=3/2$) is mediated by itinerant $e_g$ electrons (double-exchange interaction).[4,5] The transfer integral $t$ of an $e_g$ carrier is significantly affected by spin alignment as

$$t=t_0\cos(\Delta\theta/2), \tag{1}$$

where $t_0$ is the bare-transfer integral and $\Delta\theta$ is the relative angle of the neighboring $t_{2g}$ spins.[6] The magnetoresistance (MR) phenomena are explained in terms of reduction of the spin scattering of the $e_g$ carriers by the forcibly aligned $t_{2g}$ spins ($\Delta\theta\rightarrow0$). Besides the large MR effect, a variety of magnetic-field-induced phenomena were also observed such as the magnetostructure phase transition,[7] magnetovolume effect,[8] and magnetic-induced insulator-to-metal transition.[9,10]

The large MR effects are not restricted to manganese oxides. $La_{0.5}Sr_{0.5}CoO_3$ (LSCO) also shows large magnetoresistance.[11,12] Substitution of $Sr^{2+}$ for $La^{3+}$ in $La_{1-x}Sr_xCoO_3$ also causes the low-spin (LS) to high-spin (HS) or intermediate-spin (IS) of the Co site and produces carriers in a strongly hybridized band of $3d$ and oxygen $2p$ states. The carriers in $La_{1-x}Sr_xCoO_3$ may be much more itinerant, due to the increased hybridization between the Co $3d$ and O $2p$ states, than in the Mn oxides, but the strong coupling between the carriers and $t_{2g}$ spins is similarly present, resulting in ferromagnetic metal state through the double-exchange interaction.

Although many works have been carried out to understand the physics in Mn and Co oxides, the characteristics of the charge carriers are still not very clearly understood such as the carrier mobility, especially around the Curie temperature. The mobility and the carrier density in these types of materials are known to be quite low,[13] so the magnetic-field $H$ needed in Hall experiments is quite large,[14,15] where the results of the conductivity and the mobility will be affected by the strong magnetic fields.

Recent works also show that $La_{1-x}Ca_xMnO_3$ and $La_{1-x}Sr_xCoO_3$ are good candidates for the semiconductive channel layer in ferroelectric field-effect transistors (FeFETs).[16,17] So, in view of understanding the underlying and applied physics, revealing the carrier characteristics is quite important. In this letter, we report the conductivity and the drift mobility measurement of LSCO films prepared by pulsed-laser deposition by using the traveling-wave method.

The LSCO targets were prepared using the citrate process[18] with starting materials of $La_2O_3$, $SrCO_3$ and Co powder. The sintering temperature was 1100 °C. The LSCO films were prepared on fused silica substrates at 650 °C by pulsed-laser deposition using a KrF excimer laser 248 nm in wavelength. The laser energy was 200 mJ, and the flowing oxygen pressure of the chamber was 20 Pa. Finally, the LSCO films were *in situ* annealed at 650 °C in the chamber with pure oxygen of 0.5 atm. The structures of the LSCO films were studied by the x-ray $\theta-2\theta$ scan pattern as shown in Fig. 1. The LSCO films are well crystallized with a cubic structure ($a=0.381\,nm$), as reported in Ref. 19, and strongly oriented along the ⟨110⟩ direction. The chemical composition of the $La_{0.5}Sr_{0.5}CoO_3$ films, except the oxygen, was analyzed by an inductively coupled plasma (ICP) quantemeter, according to which the $La_{0.5}Sr_{0.5}CoO_3$ films show a chemical stoichiometry of 1.0:0.99:2.0 except the oxygen (the experimental error was within ±2%). The morphology and thickness of the LSCO films were examined by scanning electron microscopy (SEM). The average grain size of the LSCO films is about 40 nm, and the thickness is about 700 nm. We also find that the interface between the film and the substrate is quite sharp, indicating no serious interdiffusion occurs. This means that the interfacial defects will not affect the

a)Electronic mail: zgliu@nju.edu.cn

 © 2000 American Institute of Physics
Downloaded 20 Mar 2010 to 219.219.118.106. Redistribution subject to AIP license or copyright; see http://apl.aip.org/apl/copyright.jsp

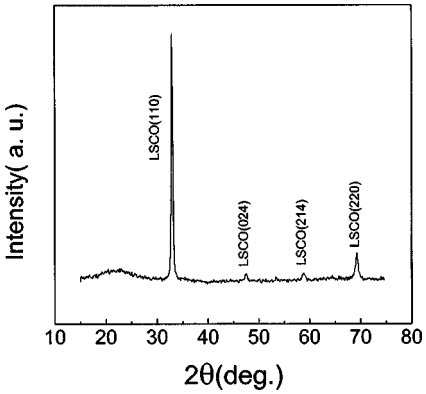


FIG. 1. X-ray $\theta-2\theta$ scan pattern for the LSCO films deposited on fused silica.

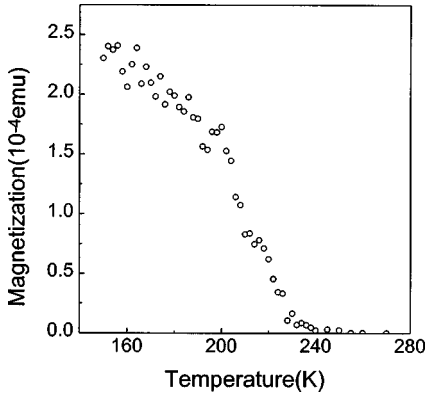


FIG. 3. Temperature dependence of the magnetization of the LSCO films.

properties of the LSCO films obviously. The magnetic moment $M$ of the sample, as a function of temperature $T$, is measured by using an Oxford vibrating sample magnetometer (VSM).

The theory of the drift-mobility measurements for the semiconductor films using the traveling-wave method was described in Refs. 20 and 21. It was schematically shown in Fig. 2. The LSCO films were placed 12 $\mu$m above the surface of the $LiNbO_3$ piezoelectric single crystal. A surface acoustic wave generated by the transducers propagates through the surface of $LiNbO_3$, supposed to be along the $z$ direction. An electric field generated by $LiNbO_3$ can be coupled into the LSCO films, which results in a dc acoustoelectric current. The drift mobility $\mu$ and the conductivity $\sigma$ can be determined by measuring the open-circuit acoustic–electric voltage $V_{av}$ and the short-circuit acoustic–electric current $I_{ae}$.[20–22]

The LSCO films were placed in a vacuum chamber cooled by liquid nitrogen. The acoustic–electric current and voltage were recorded by digit voltmeters. The dielectric constant of the LSCO film (about 5) was estimated by Kramers–Kronig (KK) analysis of the far-infrared reflective data of the LSCO film.[23]

Figure 3 shows the temperature dependence of the magnetization for the LSCO films. The Curie temperature is about 240 K, on which the LSCO film undergoes a paraferromagnetic phase transition. This result is well in agreement with that of the LSCO ceramics.[24] Figure 4 presents the temperature dependence of the resistivity for the LSCO films measured by using the traveling-wave method in Arrhenius form: $\mathrm{Ln}(\sigma T)\sim 1/T$. The LSCO film behaves like a semiconductor in all the temperature regions, as shown by the inset, similar to that reported in Ref. 25. The resistivity of the LSCO film at room temperature is about 1 $\Omega$ cm. An anomaly due to the paraferromagnetic phase transition could be observed around $T=240$ K, as indicated by the arrow. It means that the high deposition temperature which results in a semiconductor-like behavior in the resistivity does not change the spin states of the electrons in the LSCO films, which are responsible for the magnetic characteristics. The curve shows an approximately linear relationship between $\mathrm{Ln}(\sigma T)$ and $1/T$ above the Curie temperature, a thermally activated behavior, indicating that the conductive mechanism in the paramagnetic state of the LSCO film may be dominated by the small polarons. The dc conductivity due to a small-polaron-hopping process should be expressed as follows:[26,27]

$$\sigma=\frac{n_0 e^2 \omega_{\mathrm{LO}} a^2}{k_B T}\exp\left(-\frac{W_H+\frac{E_g}{2}}{k_B T}\right), \tag{2}$$

where $e$ denotes the electronic charge, $n_0\exp(-E_g/2k_BT)$ is the number of hopping small polarons per unit volume, $n_0$ being the number of low-spin Co sites per unit volume, $\omega_{\mathrm{LO}}$ is the optical-phonon frequency, $a$ is the characteristic inter-

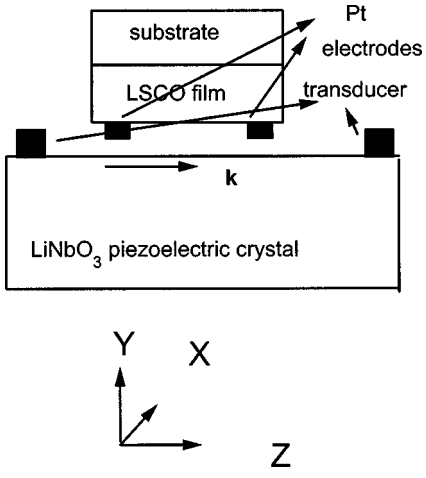


FIG. 2. Schematic drawing of the experimental configuration.

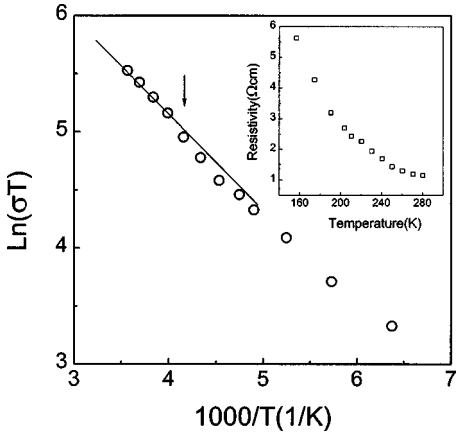


FIG. 4. Temperature dependence of the conductivity of the LSCO films, as measured by the traveling-wave method.

Downloaded 20 Mar 2010 to 219.219.118.106. Redistribution subject to AIP license or copyright; see http://apl.aip.org/apl/copyright.jsp

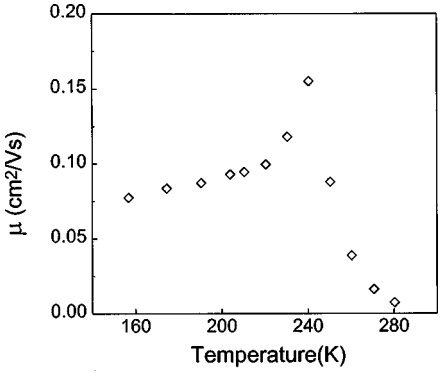


FIG. 5. Temperature dependence of the drift mobility of the LSCO films.

site hopping distance, and $W_H$ is the hopping energy of a polaron. In LSCO, the band-gap $E_g$ can be neglected in the above equation due to the higher hybridization between the Co $3d$ and O $2p$ states ($E_g/2 \ll W_H$). From Fig. 4, the thermally activated energy $W_H$ of small polarons is estimated to be about 0.075 eV, which is quite small. This result is well in agreement with that of studies on the far-infrared reflective spectra in $La_{1-x}Sr_xCoO_3$,[28] where the relative small constant of the electron-lattice interaction was obtained. The deviation of the dc conductivity from the linear behavior may be ascribed by the following reason. According to Holstein,[29] small polarons can penetrate to neighboring sites by the phonon-induced tunneling effect in addition to the hopping process. Then, the conductivity of small polarons, $\sigma$ is the sum of the hopping conductivity $\sigma_h$ and the tunneling conductivity $\sigma_t$. On the other hand, the tunneling effect of holes through the grain boundaries may give an obvious amendment to the conductivity due to the relatively small grain size. The temperature dependence of the drift mobility of the LSCO films is shown in Fig. 5. The drift mobility of the LSCO film at room temperature is about $0.01\,cm^2/V\,s$ ($\ll 1\,cm^2/V\,s$), well in agreement with the common value of polarons in a general ionic solid.[26] Below the Curie temperature, the drift mobility decreases with decreasing temperature due to the ionized-impurity scattering. Above the Curie temperature, the drift mobility decreases with increasing the temperature. In the polaronic state, the carriers are self-localized on the lattice. With decreasing temperature, the polaronic lattice collapses, and the charge carriers move easily. On the other hand, due to the paraferromagnetic phase transition at $T_C$, the carrier scattering by thermal fluctuation of the local spins decreases. Thus, the ferromagnetic spin configuration reduces the randomness of the transfer interaction, and hence, increases the carrier mobility. The $I_{ae}$ sign obtained in this work shows that holes are the majority carrier in LSCO films. Simply based on the equation $\sigma = ne\mu_h$, the hole density of the LSCO films can be estimated to be about $1\times10^{21}\,cm^{-3}$ at room temperature, which has the same order of lanthanum manganites.[14] The LSCO films have a much lower crystallizing temperature than that of lanthanum manganites (higher than 750 °C, not compatible with semiconductor technology). So, in view of semiconductor technology, LSCO films are more suitable for application as the channel layer in the FeFETs.

In conclusion, the conductivity and the drift mobility of LSCO films have been effectively measured by using the traveling-wave method. The temperature dependence of the resistivity and the drift mobility show that in the paramagnetic state the conductive mechanism of LSCO films may be dominated by the hopping process and tunneling effects. The LSCO films deposited in this work have a drift mobility of $0.01\,cm^2/V\,s$ and a hole density of $1\times10^{21}\,cm^{-3}$ at room temperature.

This work was jointly supported by a grant from the State Key Program for Basic Research of China and NSF of China (normal and special projects).

[1] S. Jin, T. H. Tiefel, M. McCormack, R. A. Fastnacht, R. Ramesh, and L. H. Chen, Science **264**, 413 (1994).
[2] G. Zhao, K. Conder, H. Keller, and K. A. Muller, Nature (London) **381**, 676 (1996).
[3] W. Archibald, J. S. Zhou, and J. B. Goodenough, Phys. Rev. B **53**, 14445 (1996).
[4] C. Zener, Phys. Rev. **82**, 403 (1951).
[5] N. Furukawa, J. Phys. Soc. Jpn. **63**, 3214 (1994).
[6] P. W. Anderson and H. Hasegawa, Phys. Rev. **100**, 675 (1955).
[7] A. Asamitsu, Y. Moritomo, Y. Tomioka, T. Arima, and Y. Tokura, Nature (London) **373**, 407 (1995).
[8] M. R. Ibarra, P. A. Algarabel, C. Marquina, J. Blasco, and J. Garcia, Phys. Rev. Lett. **75**, 3541 (1995).
[9] Y. Moritomo, H. Kuwahara, Y. Tomioka, and Y. Tokura, Phys. Rev. B **55**, 7549 (1997).
[10] H. Y. Hwang, T. T. M. Palstra, S.-W. Cheong, and B. Batlogg, Phys. Rev. B **52**, 15046 (1995).
[11] G. Briceno, H. Chang, X. Sun, P. G. Schultz, and X. D. Xiang, Science **270**, 273 (1995).
[12] J. M. Liu and C. K. Ong, Appl. Phys. Lett. **73**, 1047 (1998).
[13] N. W. Ashcroft and N. D. Meimin, *Solid State Physics* (Sounders College, Fort Worth, TX, 1976).
[14] M. Jaime, H. T. Hardner, M. B. Salamon, M. Rubinstein, P. Dorsey, and D. Emin, Phys. Rev. Lett. **78**, 951 (1997).
[15] A. Asamitsu and Y. Tokura, Phys. Rev. B **58**, 47 (1998).
[16] S. Mathews, R. Ramesh, T. Venkatesan, and J. Benedetto, Science **276**, 238 (1997).
[17] S. W. Kim and J. C. Lee, Integr. Ferroelectr. **18**, 405 (1997).
[18] J. Yin, X. S. Gao, Z. G. Liu, Y. X. Zhang, and X. Y. Liu, Appl. Surf. Sci. **141**, 71 (1999)
[19] JCPDS International Center for diffraction data (1989).
[20] R. Adler, D. Janes, B. J. Hunsinger, and S. Datta, Appl. Phys. Lett. **38**, 102 (1981).
[21] H. Fritzsche and K. J. Chen, Phys. Rev. B **28**, 4900 (1983).
[22] L. Wang, J. Yin, S. Y. Huang, X. F. Huang, J. Xu, Z. G. Liu, and K. J. Chen, Phys. Rev. B **60**, R6976 (1999).
[23] J. Yin, Z. G. Liu, X. J. Meng, H. J. Ye (unpublished).
[24] M. A. Senaris-Rodriguez and J. B. Goodenough, J. Solid State Chem. **118**, 323 (1995).
[25] P. W. Chan, W. B. Wu, K. H. Wong, K. Y. Tong, and J. T. Cheung, J. Phys. D **30**, 957 (1997).
[26] D. Emin and T. Holstein, Ann. Phys. (N.Y.) **53**, 439 (1969).
[27] I. G. Austin and N. F. Mott, Adv. Mater. **18**, 41 (1969).
[28] S. Tajima, A. Masaki, S. Vchida, T. Matsuura, K. Fueki, and S. Sugai, J. Phys. C **20**, 3469 (1987).
[29] T. Holstein, Ann. Phys. (N.Y.) **8**, 325 (1959).

**Downloaded 20 Mar 2010 to 219.219.118.106. Redistribution subject to AIP license or copyright; see http://apl.aip.org/apl/copyright.jsp**